International Journal of Electrical, Electronic and Communication Sciences
ISSN: 2517-9438
Vol:1, No:2, 2007

A New Approach to Signal Processing for DC-Electromagnetic Flowmeters

Michael Schukat

***Abstract*—**Electromagnetic flowmeters with DC excitation are used for a wide range of fluid measurement tasks, but are rarely found in dosing applications with short measurement cycles due to the achievable accuracy. This paper will identify a number of factors that influence the accuracy of this sensor type when used for short-term measurements. Based on these results a new signal-processing algorithm will be described that overcomes the identified problems to some extend. This new method allows principally a higher accuracy of electromagnetic flowmeters with DC excitation than traditional methods.

***Keywords*—**Electromagnetic Flowmeter, Kalman Filter, Short Measurement Cycles, Signal Estimation

I. Introduction

ELECTROMAGNETIC flowmeters (EMFMs) are non-invasive devices that measure the velocity and consequently the flow of a conductive fluid like water or slurry through a pipe. They are founded on Faraday's law of induction, whereby an electrical field E is induced in a moving liquid in the presence of a magnetic field B (see Figure 1). E is perpendicular both to B and the fluid velocity v [1].

An EMFM consists of a pair of coils that yield a uniform magnetic field B vertical to the flow channel. Two opposite electrodes inside the pipe allow measuring the resulting induced voltage U_N with

$$U_N = kB \cdot l \cdot \bar{v} \tag{1}$$

$\bar{v}$ represents the average fluid velocity, l is the width of the pipe and k is a calibration constant.

U_N is overlaid by an unwanted DC-component $U_G(t)$, which is the result of electrochemical effects between the electrodes and the fluid. In order to separate both components the magnetic field is modulated.

A DC-EMFM generates a bipolar magnetic field with a square waveform that has a frequency of a quarter of the mains supply frequency (e.g. 12.5 Hz or 15 Hz) [2]. In order to calculate the flow-proportional component $U_N(t)$, the electrode signals during the two periods of an excitation cycle with a constant magnetic field are integrated separately and subtracted from each other (see Figure 2). Since $U_G(t)$ is assumed to be constant over the entire excitation cycle with the length T_P, the resulting value will only depend on $U_N(t)$ and additional AC components induced by the mains voltage. The latter will be compensated, if each integration window has the length $0.25 * T_P$.

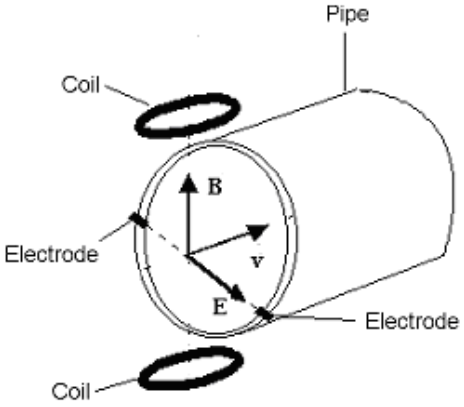

Figure 1: Cross-section of an EMFM.

DC-EMFMs are mainly used for continuous flow measurements. The measurement error here has been reported to be as low as 0.3 percent. In contrast to this it has been shown that this type of sensor causes significantly higher errors when used for short-term measurements, which makes DC-EMFMs unsuitable for dosing applications. This paper will examine a number of problems that affect the accuracy of this sensor type and will describe a new signal processing technique that overcomes these problems to some extend.

II. Problem Analysis

A. Electrochemical Effects

Each electrode and the fluid form a simple galvanic element. Consequently, surface reactions take place, whereby an exchange of electrons and a charge redistribution occurs. This results in a complex electrolytic double-layer structure. The exact nature of this process depends both on the fluid (e.g. the ions dissolved) and on the surface structure of the electrodes [3]. $U_G(t)$ is basically the result of structural

Dr. Michael Schukat is a lecturer with the Department of Information Technology, National University of Ireland, Galway (phone: +353-91-512419; fax: +353-91-750501; e-mail: michael.schukat@nuigalway.ie).

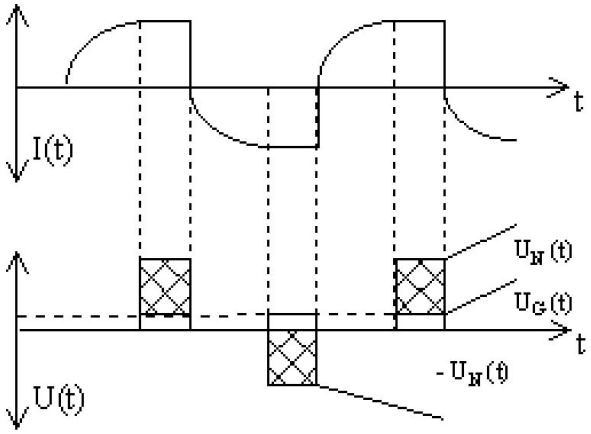

Figure 2: Coil excitation current I(t) (top) and resulting electrode signal U(t) during the integration period assuming both a constant fluid velocity and offset voltage $U_G(t)$ (bottom).

differences between both electrode surfaces and the resulting different cell voltages. Although $U_G(t)$ is being considered to be a DC component, it is likely to change spontaneously due to temporal deposits like dirt or discharged ions on the electrode surfaces that build up slowly over time, until they are torn away by the moving fluid. The result is a sudden drift of $U_G(t)$, which cannot be predicted or compensated through the integration and differencing process as described in section I. Assuming that $U_G(t)$ has a constant slope A_S due to rebalancing electrochemical processes on one electrode, the uncompensated offset voltage adds up to a value

$$\frac{A_S T_P^2}{2} \tag{2}$$

per excitation cycle, which is misinterpreted as a flow-proportional component. This factor can cause a significant measurement error during a short-term measurement.

A second problem is associated with electrostatic noise effects: The double layers along each electrode can be seen as a series of two capacitors C_L and C_R. The combined capacitor voltage U_C can be calculated with

$$U_C = \frac{Q(C_L + C_R)}{C_L C_R} \tag{3}$$

with an electrical charge Q [4]. Fluids with a low conductivity cause a weak and diffuse double layer structure along the electrodes that is constantly disturbed by the moving fluid, affecting therefore C_L and C_R. This results in an additional noise signal that overlays $U_N(t)$. Experimental results have shown that the noise signal transforms gradually from a colored spectrum to a white spectrum with increasing fluid conductivity. The energy of the noise depends both on the fluid conductivity and fluid velocity.

B. Asymmetric Flow Signals

In order to work correctly, the DC-EMFM signal-processing algorithm as described in section I requires that

$$\sum_{i=0}^{2n} \int_0^{\frac{1}{4}T_P} U_N\left(t + \frac{iT_P}{2} + \frac{1}{4}T_P\right) dt = \sum_{i=0}^{2n} \int_0^{\frac{1}{4}T_P} U_N\left(t + \frac{iT_P}{2}\right) dt \tag{4}$$

whereby n is the number of excitation cycles during the flow measurement. This symmetry is given if the fluid velocity is constant over time, but is not necessarily there in situations where the flow is pulsating. Displacement pumps that are often found in dosing applications cause pulsating flows.

The otherwise resulting measurement error depends on the duration of the measurement, the shape of the pulsation wave and the pulsation frequency. Since the coil excitation and the pump are not synchronised with each other, the initial phase shift between both is another variable to be taken into account.

C. *The Temporal Resolution of DC-EMFMs*

In a dosing application, the fluid flow is stopped, once a specific volume has been reached. A DC-EMFM on the other hand provides only a flow measurement value every T_P seconds. As a result, the desired volume is hardly every hit, but is more likely to be exceeded. The resulting measurement error depends on the fluid velocity gradient before the desired fluid volume is reached and the initial phase shift between the coil excitation and the start of the dosing process.

III. The Proposed Algorithm

Figure 3 shows an idealised DC-EMFM signal with known segments f_i that have boundary points a_i and e_i. During one excitation period T_P the sensor provides two segments f_{2i} and f_{2i+1} of the electrode signal during periods with alternating but constant magnetic field. Each segment has the length $0.25 * T_P$. The proposed envelope calculation (EC-) algorithm interpolates the missing signal between two segments f_{2i+x} and f_{2i+x+2} using cubic Hermite polynoms p_{2i+x} with

$$p_n(t) = \left[t^3 t^2 t^1 t\right] \cdot M_H \cdot \begin{bmatrix} f_n(e_n) \\ f_{n+2}(a_{n+2}) \\ \dot{f}_n(e_n) \\ \dot{f}_{n+2}(a_{n+2}) \end{bmatrix} \tag{5}$$

and with some base matrix M_H [5]. $p_n(t)$ is only defined

between it's boundaries e_n and a_{n+2} and is 0 otherwise.

The upper and lower envelope between two points in time t_a and t_e can be written as

$$u_{(t_a,t_e)}(t) = \sum_{k\in K} f_{2k}(t) + p_{2k}(t) \tag{6}$$

and

$$l_{(t_a,t_e)}(t) = \sum_{k\in K} f_{2k+1}(t) + p_{2k+1}(t) \tag{7}$$

with suitable index values k. The integrated flow-proportional signal component over that period of time can be calculated with

$$DFM_1(t_a,t_e) = \int_{t_a}^{t_e} \left[u_{(t_a,t_e)}(t) - l_{(t_a,t_e)}(t)\right] dt \tag{8}$$

Figure 3 shows that until some moment e_{2i+5} the algorithm provides only a complete envelope until e_{2i+4}. A preliminary estimation of the flow over the last half excitation period can be done through an estimation of the offset voltage component $s_{2i+5}(t)$ between e_{2i+3} and e_{2i+4}. This offset component is geometrically between the upper and the lower envelope. Based on the assumption that $s_{2i+5}(t)$ is either constant or has a linear drift, it can be approximated by a first-degree polynomial, that in turn allows the estimation of the offset voltage $v_{2i+5}(t)$ between e_{2i+4} and e_{2i+5}. The overall integrated flow signal can be calculated with

$$\begin{aligned} DFM_2(t_a,e_n) &= DFM_1(t_a,e_{n-1}) \\ &+ 2\int_{e_{n-1}}^{e_n} \left|v_n(t) - (p_{n-2}(t) + f_n(t))\right| dt \end{aligned} \tag{9}$$

The latter preliminary estimation term can be replaced with $DFM_1(e_{n-1},e_n)$ after another coil excitation.

The algorithm provides flow measurement values with a rate of $2/T_P$ or every 40 ms based on an excitation frequency of 12.5 Hz. This can be increased by a prediction of the flow signal component until the next measurement value is available at a moment e_{n+1}. The approach takes advantage of the fact that the flow signal DF itself can be approximated:

$$\begin{aligned} DF_{(t_a,e_n)}(t) &= u_{(t_a,e_{n-1})}(t) - l_{(t_a,e_{n-1})}(t) \\ &+ 2\left|\, v_n(t) - (p_{n-2}(t) + f_n(t))\,\right| \end{aligned} \tag{10}$$

Depending on the fluid pump and the dosing valve being used the resulting flow signal is either linear or periodically

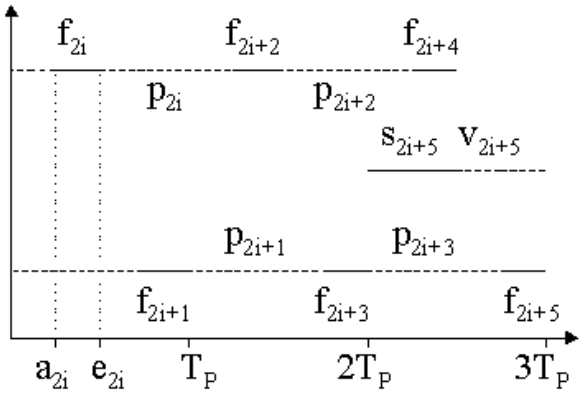

Figure 3: The envelope of the electrode signal.

oscillating. Linear flow signals can be predicted by applying an extrapolation algorithm, while a pulsating flow can be handled by a correlator, whereby the flow signal over the last number of seconds will be compared against the latest known segment of the flow signal. If a match based on some threshold value is found, the stored signal following the match will be used as a prediction. In any case the resulting value is only used temporarily and will be replaced with corrected terms as defined in Equation 8 and Equation 9 after another coil excitation.

The overall effect of this algorithm can be seen in Figure 4. At some moment e_{2i} the algorithm calculates flow values for areas (A) and (B) according to Equation 9 and performs a flow prediction for (C). Half an excitation period later the value for (B) will be corrected by calculating $DFM_1(e_{2i-1},e_{2i})$, while the flow prediction (C) will be replaced with a value calculated similar to the (B) component during the previous iteration.

In order to take account of noise effects as described in section II.A. a Kalman smoothing algorithm has been implemented [6]-[7]. It is based on the system model

$$\begin{bmatrix} x_0(t_{k+1}) \\ x_1(t_{k+1}) \end{bmatrix} = \begin{bmatrix} 1 & T \\ 0 & 1 \end{bmatrix} \cdot \begin{bmatrix} x_0(t_k) \\ x_1(t_k) \end{bmatrix} + \begin{bmatrix} 0 & 0 \\ 0 & 1 \end{bmatrix} \cdot \begin{bmatrix} 0 \\ w_1(t_k) \end{bmatrix} \tag{11}$$

and the observation model

$$[z_0(t_k)] = [1 \quad 0] \cdot \begin{bmatrix} x_0(t_k) \\ x_1(t_k) \end{bmatrix} + [v_0(t_k)] \tag{12}$$

T is the sampling interval, while $w_1(\cdot)$ represents a white noise process with variance σ_w, that drives the system model. The observation model contains another white noise process $v_0(\cdot)$ with variance σ_v that represents the measurement error. The filter parameters $x_0(\cdot)$ and $x_1(\cdot)$ in Equation 11

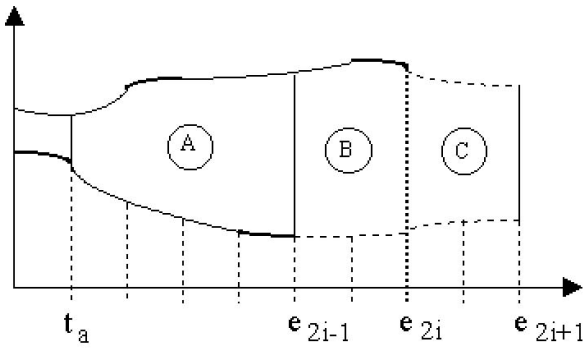

Figure 4: Segments of various certainties.

are used to parameterise the Hermite polynoms as defined in Equation 5.

An AC component as induced by the mains voltage can be principally compensated using an enhanced system model, but it has been shown that this extension makes the smoothing algorithm computationally very costly. Instead, a 50 Hz notch filter has been implemented.

IV. Experimental Results

The algorithm has been tested using a number of simulations that were based on EMFM signals representing constant and pulsating fluid flows.

Figure 5 shows the EC-algorithm being applied to a simulated electrode signal. The graph on the left hand side represents an electrode signal that combines a linear increasing offset voltage with a drift of $33\mu V\,s^{-1}$ and a noise process with a variance of $3\mu V$. The graph on the right hand side plots the output of the EC-algorithm. It shows that the linear drift is completely compensated. The maximum measurement error that has been found during all simulations based on the above parameters was about 8 percent of the error produced by a conventional DC-EMFM signal analysis.

Figure 6 compares a pulsating flow signal $U_N(t)$ and the output of the EC-algorithm over a period of four seconds. $U_N(t)$ has been overlaid by a constant offset and a noise process with a variance of $3\mu V$ before being processed. The graph shows the capability of the EC-algorithm to reconstruct pulsating flow signals. The maximum measurement error that was found in all simulations based on these parameters was 0.25 percent in comparison to 0.75 percent using the conventional DC-EMFM signal processing method.

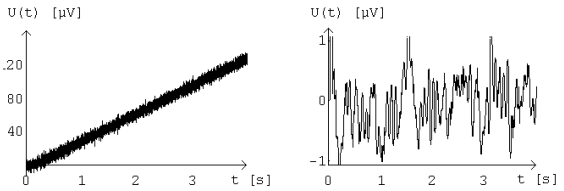

Figure 5: Offset and noise compensation of the algorithm.

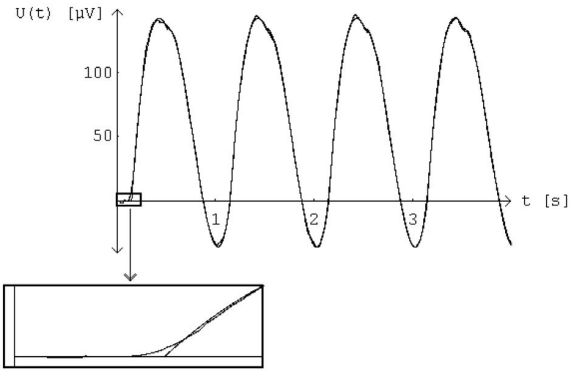

Figure 6: Original versus reconstructed signal based on a pulsating flow.

Further tests have shown that the method cannot reconstruct properly fluid signals that contain spectral frequency components beyond 0.5 T_P^{-1} Hz or 6.25 Hz for an excitation period length of 80 ms, therefore restricting the versatility of this algorithm. This frequency limitation is the consequence of the Nyquist theorem applied to this problem [8].

V. Conclusion

The EC-algorithm provides a new and effective method to improve the accuracy of DC-EMFMs by reconstructing the flow signal and by compensating distortions based on noise and offset voltages. The algorithm requires a high-performance processor due to the implemented Kalman filter.

The method is limited to frequency-limited flow-signals that are not necessarily given if a displacement pump is used.

Modifications to the system model are required if fluids with a low conductivity are used, since a colored noise spectrum needs to be considered in this case.

References

[1] Bonfig, K.W. (1970). Einfluesse auf die Nutzspannung bei der induktiven Durchflussmessung, *Archiv fuer technisches Messen*, Blatt V 1249 – 8, pp. 145-150.

[2] Polo, J., Pallas-Areny, R., Martin-Vide, J.P. (2002). Analog Signal Processing in an AC Electromagnetic Flowmeter, IEEE Transactions on Instrumentation and Measurement, Vol. 51, No. 4, pp.793-797

[3] Hamann, C. H., Hamnett, A., Vielstich, W. (1998). Electrochemistry, Wiley VCH, ISBN 3527290958, pp. 153-154

[4] Luettgens, G. (1989). Understanding and Controlling Static Electricity, Expert Verlag, ISBN 3816905102, pp. 50-53

[5] Foley, J. (1992). Computer Graphics – Principals and Practice, Addison-Wesley Publishing Company Inc., ISBN 0201121107, pp. 517-520

[6] Maybeck, P.S. (1979). Stochastic Models, Estimation, and Control, Volume 1, Academic Press, pp. 203-215

[7] Maybeck, P.S. (1982). Stochastic Models, Estimation, and Control, Volume 2, Academic Press, pp. 9-15

[8] Oppenheim, A.V. (1984). Signals and Systems, Prentice Hall Inc., ISBN 0138111758, pp. 440-442